Polyurethane foam/nano hydroxyapatite composite as a suitable scaffold for bone tissue regeneration

M. Meskinfam[a,b], S. Bertoldi[a,c], N. Albanese[a], A. Cerri[a], M.C. Tanzi[c], R. Imani[d], N. Baheiraei[e], M. Farokhi[f], S. Farè[a,c,*]

[a] *Department of Chemistry, Materials and Chemical Engineering "G. Natta" Politecnico di Milano, Milano, Italy*
[b] *Lahijan Branch, Islamic Azad University, Lahijan, Iran*
[c] *INSTM, Consorzio Nazionale di Scienza e Tecnologia dei Materiali, Local Unit Politecnico di Milano, Italy*
[d] *Department of Biomedical Engineering, Amirkabir University of Technology, Tehran, Iran*
[e] *Department of Anatomical science, Faculty of Medical Sciences, Tarbiat Modares University, Tehran, Iran*
[f] *National Cell Bank of Iran, Pasteur Institute of Iran, 69 Tehran, Iran*

In bone tissue regeneration, the use of biomineralized scaffolds to create the 3D porous structure needed for well-fitting with defect size and appropriate cell interactions, is a promising alternative to autologous and heterologous bone grafts. Biomineralized polyurethane (PU) foams are here investigated as scaffold for bone tissue regeneration. Biomineralization of the foams was carried out by activation of PU surface by a two steps pro-cedure performed for different times (1 to 4 weeks). Scaffolds were investigated for morphological, chemico-physical and mechanical properties, as well as for in vitro interaction with rat Bone Marrow Mesenchymal Stem Cells (BMSCs). Untreated and biomineralized PU samples showed a homogenous morphology and regular pore size (average Ø = 407 μm). Phase and structure of formed calcium phosphates (CaPs) layer onto the PU foam were analyzed by Fourier Transform Infrared spectroscopy and X-ray diffraction, proving the formation of bone-like nano hydroxyapatite. Biomineralization caused a significant increase of mechanical properties of treated foams compared to untreated ones. Biomineralization also affected the PU scaffold cytocompatibility providing a more appropriate surface for cell attachment and proliferation. Considering the obtained results, the proposed scaffold can be considered suitable for bone tissue regeneration.

Keywords:
Porous scaffold
Polyurethane
Nano hydroxy apatite
Bone
Tissue engineering
Biomineralization

1. Introduction

Due to the large number of patients suffering of bone defects caused by trauma, tumor or diseases, in recent years, numerous investigations are in progress, making efforts on the development of new materials [1–4] and processing techniques [5,6] for bone tissue regeneration. Nevertheless, in spite of the intense researches, there is a big gap between the ongoing in vitro studies and the clinical innovative approaches. Nowadays, in clinical therapies for bone regeneration, autologous bone, allografts, demineralized heterologous bone or bone substitutes are used. Although autografts represent an excellent option, thanks to their osteoconductivity, osteoinductivity and non-immunogenicity [7], their use is limited by donor shortage and donor site morbidity [8]. In addition, allograft presents the risk of immunological problems and disease transmission [9]. Therefore, a bone defect reconstruction can greatly benefit from alternative sources, especially from engineered scaffolds with the capability of integration into the surrounding bone tissue. In order to allow the regeneration of a natural bone tissue, the scaffold should possess a suitable surface chemistry to support cell adhesion, proliferation, migration and growth. In addition, it should act as a biocompatible template for osteoprogenitor cell growth, promote the differentiation of mesenchymal stem cells (MSCs) into osteoblast phenotype and support production, organization and maintenance of the extracellular matrix. Finally, scaffolds are required to have highly interconnected pores with adequate size to promote cell migration and nutrient distribution [10]. The use of natural or synthetic polymers for bone tissue regeneration is extremely appealing due to the possibility of processing them into three-dimensional (3D) structures [11]. Collagen [12], chitosan [13], gelatin [14], hyaluronic acid [15] and alginate [13] represent the most promising natural polymers for bone tissue regeneration. However, despite their excellent biocompatibility, the use of such polymers by themselves is limited by significant drawbacks such as the weak mechanical properties and poor processability. To improve the mechanical properties of the structure,

* Corresponding author at: Department of Chemistry, Materials and Chemical Engineering "G. Natta" Politecnico di Milano, Milano, Italy.
E-mail address: silvia.fare@polimi.it (S. Farè).

Published Journal Article available at: http://dx.doi.org/10.1016/j.msec.2017.08.064

composite scaffolds based on natural polymers as matrix and reinforced with inorganic particles are under investigation [16–18,61]. Synthetic biodegradable polymers are proposed for bone tissue regeneration as well, including polydioxanone [19], polyorthoesters [20–23], polyanhydrides [19], poly (α-hydroxyesters) [20–23], poly (lactide-*co*-glycolide) [21–23] and polyurethanes [4,24]. However, balancing between in vivo degradation and tissue regeneration is not easily achievable, because it depends on different variables in clinical conditions, such as shape and size of bone defect, release of acidic degradation products that may lead to non-physiological inflammatory response, and functional loading, which affects bone regeneration and remodeling.

An interesting alternative to biodegradation is biointegration. It can be obtained by using polymers with a slow degradation rate, specifically designed to fulfil all the key requirements. Scaffolds could be effectively used to restore large defects in such a way to prevent tissue collapse and sustain the newly forming tissue for longer time than conventional biodegradable polymers. In this perspective, polyurethanes (PU) show a range of mechanical and morphological properties significantly larger than other medical-grade biodegradable polymers [4,25,26]; in particular, promising results have been obtained with polyurethane foams both in vitro [27–31] and in vivo animal models (rat, sheep) [28,32] for bone tissue regeneration. In the last years, crosslinked PU foams with slow degradation rate and controlled range of pore size, open porosity and mechanical properties were developed [4,33]. PU foams with different range of hydrophilicity [34], surface modified with proteins [35] and composites [34] have been investigated.

According to some researches [36,37], one of the important requirements for a synthetic material to show a bone-bonding behaviour is the formation of a calcium phosphate interface similar to bone apa-tite. On the other hand, the presence of an apatite-like layer on the scaffold surface is the sign of a positive biological response from the host tissues. Hence, it is expected that a material holding that kind of coating would present a bioactive behaviour after implantation [38]. Bioactive glass is such a material that has the ability to form an apatite-like layer on the polymer surface and therefore bonding to living tissues [39]. In the formation mechanism of this layer, silanol groups play an important role [40,41]. Several studies [42–44] report investigation for mimicking the in vivo natural processes leading to CaPs deposition so to allow an in vitro mineral phase deposition onto polymeric 3D porous scaffolds. However, the main problem is providing the adequate che-mical conditions on the substrate [42–44], so to induce the precipita-tion of CaPs phase [38,62,63]. CaPs coatings have been produced on a different kinds of materials such as metals [42,43], non-biodegradable polymers [43,44], bioinert ceramics [43], and even natural polymers like bamboo [45].

Polyurethanes can undergo calcification in vivo [46] and, if this represents an important problem for cardiovascular applications, urinary prosthesis and intrauterine contraceptive devices, it becomes beneficial for bone substitution. In fact, the deposition of CaPs onto the polyurethane surface can promote osteoconductivity and bone bonding [47].

In the present study, a treatment based on calcium and phosphate ions as precursors for the nucleation and growth of calcium phosphate on the pore wall of PU porous scaffold was performed (Fig. 1) and investigated. After that, the adhesion and proliferation of Bone Marrow Mesenchymal Stem Cells (BMSCs) isolated from rat femora and tibia, were investigated on the biomineralized PU foam.

2. Materials and methods

2.1. Polyurethane foam synthesis

The poly-ether-urethane (PU) foam was synthesized according to a previously optimized production process [4,34,48]. The synthesis process consisted in a one-step bulk polymerization, performed by gas foaming reaction. The reaction mixture was prepared in a polypropylene beaker by adding an ad hoc prepared poly-ether-polyol mixture [49,59], distilled water as expanding agent (2% w/wpolyol), Fe-acetylacetonate as reaction catalyst (FeAA, 0.001% w/wpolyol) and 4-4′-methylene diphenyl diisocyanate prepolymer (Desmodur PF, Bayer Germany, NCO = 5.476 mmol/g). The synthesis was performed using a non-stoichiometric ratio of OH/NCO = 100/133, with an isocyanate excess. The reaction mixture was mixed by a mechanical stirrer (ALCW750, MAVER) at 2000 rpm for 1 min. After mixing, 75 g of the reaction mixture were poured inside a custom-made poly (methyl methacrylate) mold (V = 500 cm^3, Fig. 1). The mold was firmly tight so to allow a confined expansion process, thus obtaining foams homogeneously expanded, with controlled and reproducible properties. The mold was kept at room temperature (R.T.) for 72 h to allow for the complete gas foaming reaction. At completed reaction, the foam was manually removed from the mold; the compact external skin (thick-ness = 1 cm) was gently removed, so to obtain a homogeneous porous structure. The foam was finally post-cured at R.T. for 3 days. For morphological, physical and mechanical characterization and in vitro biological investigation tests, cylindrical samples (Ø = 10 mm, h = 4 mm) were obtained by manually punching PU foam slices. Samples were immersed in pure ethanol for 48 h, to allow the complete removal of possible low molecular weight products that could affect the PU foam cytocompatibility, and subsequently let dry at R.T. for 24 h before further characterization.

2.2. Biomineralization process

Biomineralization treatment (Fig. 1) was performed on PU foam specimens as substrates for nucleating the apatite film. PU samples were immersed in $CaCl_2 \cdot 2H_2O$ (Sigma-Aldrich) 0.5 M for 3 days at 37 °C and after washing with distilled water, soaked in $Na_2HPO_4 \cdot 12H_2O$ (Sigma-Aldrich) 0.3 M for 3 days at 37 °C. The aim of this step was the initial nucleation of calcium phosphate layer due to a chemical reaction between Ca and P ions on the PU scaffold surface. After that, biomineralization was carried out by immersion of the PU samples in 1.5 SBF for different time points (t = 1, 2, 3 and 4 weeks). 1.5 SBF contains a concentrations of Ca^{2+} and PO_4^{3-} ions 1.5 times larger than SBF that presents an ion concentration nearly equal to human blood plasma. The 1.5 SBF solution was prepared using the Kokubo et al. [43] protocol, by dissolving NaCl, $NaHCO_3$, KCl, $K_2HPO_4 \cdot 3H_2O$, $MgCl_2 \cdot 6H_2O$, $CaCl_2$ and Na_2SO_4 (Sigma-Aldrich) in distilled water (Table 1), buffered with tris (hydroxymethyl) aminomethane, $(CH_2OH)_3CNH_2$, and adjusting pH at 7.4 at 37 °C by stirring the solution and titrating it with HCl. Each week, the 1.5 SBF solution was changed to preserve 1.5 SBF constant ion concentrations during the nucleation procedure. Four group samples (n = 20 each) were prepared considering different immersion times in 1.5 SBF (1, 2, 3 and 4 weeks) and named PU-1W, PU-2W, PU-3W and PU-4W, respectively.

2.3. Scaffold morphological characterization

For morphological evaluation, PU foam specimens before and after HA nucleation treatment were mounted on aluminum stubs, gold sputter-coated (Sputter Coater S150B, Edward) and observed by Scanning Electron Microscopy (SEM, StereoScan 360 Cambridge) at 10 kV. Deeper investigation on the morphology of nucleated calcium phosphate layer on PU foams at the considered time-points was performed by SEM (KYKY-EM3200) at 26 kV.

2.4. Physical characterization

For physical characterization, density and water uptake tests were carried out. Density analysis was performed on untreated and treated PU foam specimens (Ø = 10 mm, h = 4 mm, n = 5). EN ISO 845

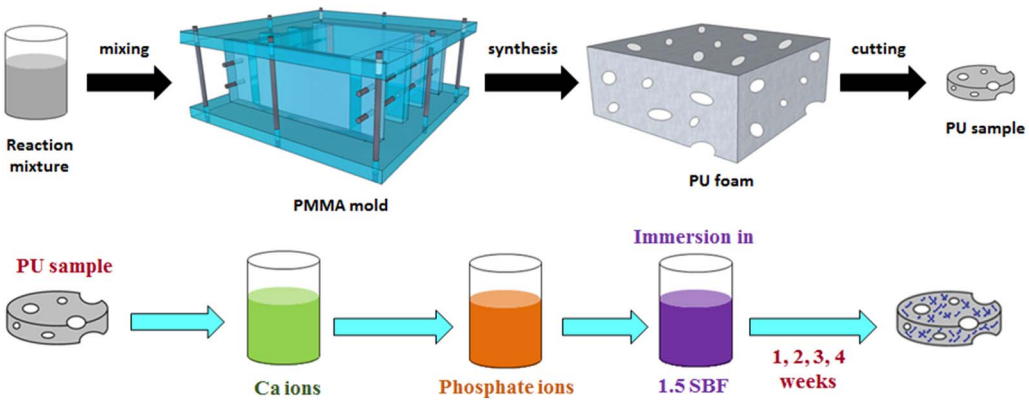

Fig. 1. Schematic diagram of polyurethane foam/nano hydroxyapatite composite fabrication.

Table 1
Ion concentrations of blood plasma, SBF and 1.5 SBF (mM) [43].

	Na^+	K^+	Ca^{2+}	Mg^{2+}	Cl^-	HCO_3^-	HPO_4^{2-}	SO_4^{2-}
Blood plasma	142.0	5.0	2.5	1.5	103.0	27.0	1.0	0.5
SBF	142.0	5.0	2.5	1.5	148.8	4.2	1.0	0.5
1.5SBF	142.0	5.0	3.75	1.5	148.8	4.2	1.5	0.5

standard practice was applied for density analysis by weighing and measuring the specimens after conditioning for 24 h at 25 °C.

Water uptake kinetic for untreated and treated PU foam specimens (= 10 mm, h = 4 mm, n = 4) was evaluated by immersion at 37 °C of each specimen in 2 ml of distilled water. At each time point (t = 15 min, 30 min, 1, 2, 3, 6, 24 h and every 24 h until the absorption plateau was reached) samples were blotted with laboratory paper to remove liquid in excess, and weighed. Water uptake, WU (%), was calculated according to the Eq. (1):

$$WU\,[\%] = \frac{w_t - w_0}{w_0} \times 100 \quad (1)$$

where w_0 is the dry weight and w_t is the wet weight at each time point.

The values of density and WU% were reported as mean ± standard deviation at each time-point of the related material sample (i.e., PU, PU-1W, PU-2W, PU-3W, and PU-4W).

2.5. Chemical characterization

Chemical characterization was performed by FT-IR and XRD analyses. The functional groups of calcium phosphate layer nucleated on PU foam at the considered time-points were evaluated by Fourier Transform Infrared spectroscopy (FT-IR, Nicolet 5700 FTIR Spectrometer, Thermo®). KBr pellet were prepared to analyze the CaPs powders obtained from the treated PU foams. Briefly, the CaPs powder was gently scratched from the surface of the treated PU foam sample with a metal spatula. Approximately 2–3 mg of CaPs powder were accurately mixed with 98 mg of dried KBr powder, homogenized, finely pulverized, and put into a pellet-forming die, so to obtain transparent pellets for recording FT-IR spectra.

The crystal structure of the CaPs layer precipitated on PU foam at the different treatment times was investigated by X-ray diffractometer (XRD, Philips Analytical®). CaPs powder was smoothen and put in the sample holder and XRD patterns were recorded at 2θ ranging from 2 to 70°.

2.6. Mechanical characterization

Compression mechanical tests were performed on cylindrical samples of untreated and treated PU foam (n = 3, Ø = 10 mm, h = 4 mm) with a Dynamic Mechanical Analyzer (DMA Q800, TA Instruments). Tests were performed on hydrated samples, i.e. specimens hydrated in distilled water for 72 h, until the WU% plateau was reached. During the test, samples were maintained hydrated using a custom made chamber filled with distilled water. Following an isotherm at 37 °C for 5 min and a preload of 0.005 N, load was applied up to 50% with a strain ramp of 2.5%/min and then removed with a strain ramp of 5%/min. Elastic modulus (E), maximum stress (σ_{max}, at 50% deformation), residual deformation (ε_r), and hysteresis area, significant for energy dispersion, were drawn from σ/ε curve elaboration. The values of the considered mechanical parameters were expressed as average value ± standard deviation for each PU foam sample.

2.7. In vitro cytocompatibility tests

2.7.1. Bone marrow mesenchymal stem cells (BMSCs) isolation

Bone marrow mesenchymal stem cells (BMSCs) were isolated from rat. Briefly, 8 week old rat was sacrificed according to the ethics committee guidelines for laboratory animals approved by Tehran University of Medical Sciences (Tehran, Iran). First, the cancellous bone of rat femur and tibia was removed, and washed 3–5 times with PBS. Then, the bone marrow was flushed out using Dulbecco's Modified Eagle Medium (DMEM) supplemented with 1% penicillin/streptomycin and 1% L-glutamine. Cells were collected in a 25 cm^2 culture flask containing DMEM with 10% (v/v) fetal bovine serum (FBS), and incubated at 37 °C and 5% CO_2. Cells were allowed to attach overnight and then the non-adherent cells were removed. The culture medium was changed twice a week and cells were split after reaching 70–80% confluence.

2.7.2. In vitro interaction with BMSCs

Samples of untreated PU foam and PU-W4 (Ø = 10 mm; h = 4 mm; n = 5) were placed in a 48 multiwell culture plate, treated with demineralized water overnight, and then sterilized with ethylene oxide. BMSCs (cell density = 5 × 10^3 cells/well) were seeded on each scaffold, considering cells cultured on Tissue Culture Polystyrene (TCPS) as control. Samples were incubated at 37 °C and 5% CO_2 up to 7 days of culture. The cytocompatibility of the prepared scaffolds was assessed using MTT (3-[4, 5-dimethylthiazol-2-yl]-2, 5-diphenyltetrazolium bromide) colorimetric assay at 1, 3, 7 days post seeding. In order to assess the cell viability at each time point, 100 µl MTT solution (5 mg/ml in PBS) were added to each well and incubated for 4 h. Then, the MTT solution was removed and the formazan precipitates were dissolved in isopropyl alcohol. The absorbance at 570 nm was measured using a microplate reader (ELISA reader, ELX808, BioTek). The absorption value of the MTT solution alone was subtracted from the values related to seeded PU samples and control. The relative cell viability (compared to TCPS, used as control) was calculated as follows:

$$\text{Relative cell viability}\,(\%) = (\text{ODs}/\text{ODc}) \times 100 \quad (2)$$

where ODs and ODc represent optical density of sample and control, respectively. PU and PU-4W samples were observed by SEM

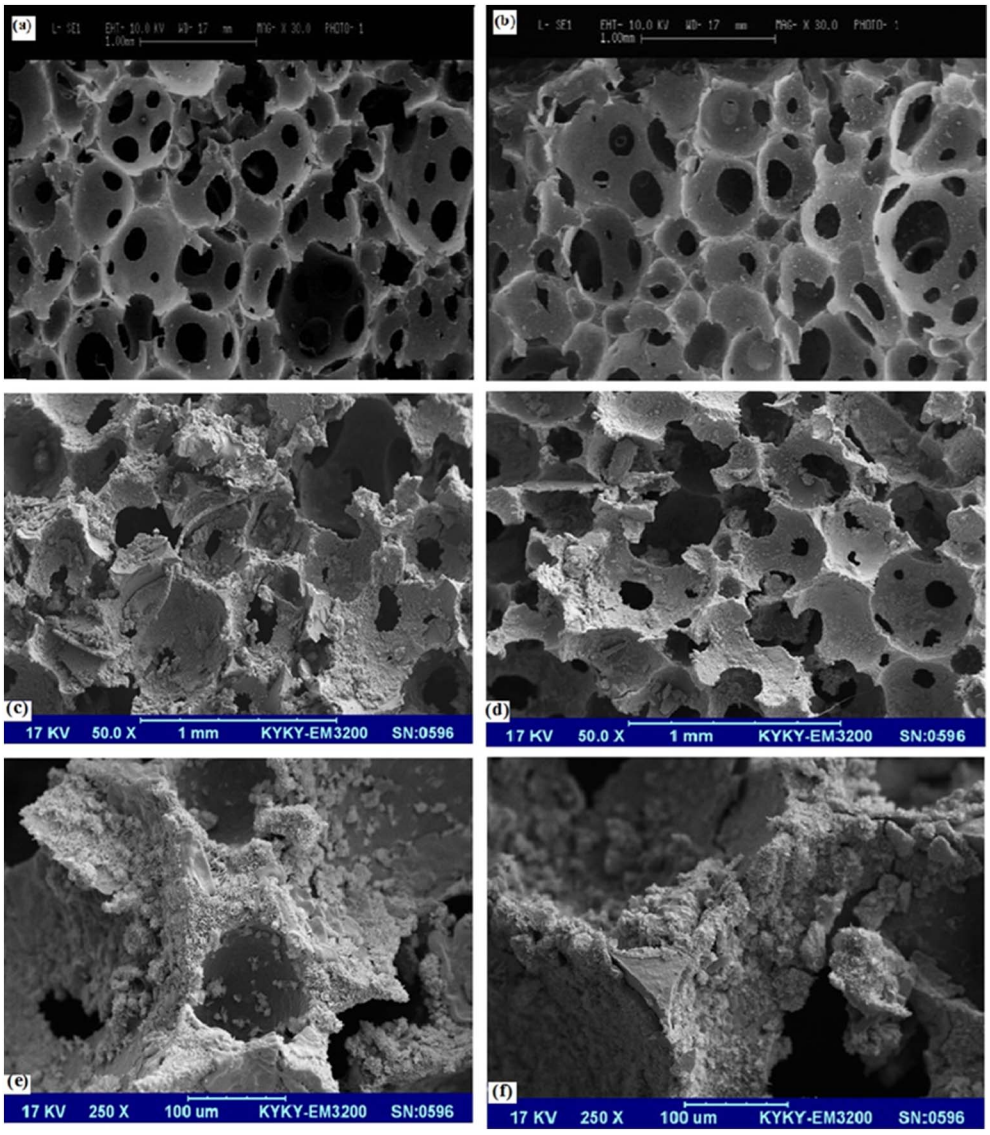

Fig. 2. SEM micrographs of the untreated PU foam a) surface; b) cross-section and PU-4W c, e) surface and d, f) cross-section. Scale bar: 1 mm (a–d), 100 μm (e–f).

(Serontechnologies-AIS2100), to evaluate BMSCs morphology and distribution on the foam surface. At each time point (1, 3 and 7 days), scaffolds were washed with PBS, fixed in 2.5% glutaraldehyde solution for 1 h, dehydrated through a series of ethyl alcohol solutions in distilled water (from 10 to 100% ethyl alcohol) and air dried. Samples were sputter coated with gold and observed at 20 kV, at different magnifications.

2.7.3. Alkaline phosphatase (ALP) activity

BMSCs were seeded on the scaffolds placed into a 24-well TCPS, at a cell density of 2×10^3 cells/well. The commercial kinetic kit (Pars Azmun, Iran) was used to get information on the ALP activity. At 3, 7, 14 days after seeding, 10 μl of supernatant were removed from each well and mixed with 800 μl of diethanolamin (1.0 Mol/l)/magnesium chloride (0.5 mMol/l) solution, and 200 μl of *p*-nitrophenolphosphate (10 mMol/l). The ALP activity was indicated by conversion of *p*-nitrophenylphosphate to *p*-nitrophenol at 37 °C and pH 9.8. The absorbance variations were monitored at 405 nm and 37 °C using a microplate reader (Bio-Rad, Hercules, CA, USA). For each time point, three replicates were considered.

2.8. Statistical analysis

The obtained results were reported as mean and standard deviation values. Data were analyzed by the Student *t*-test with significance level $p = 0.05$. Statistical analysis was carried out using SPSS software (v 17.0; IBM New York, NY, USA).

3. Results and discussion

3.1. Scaffold design

Due to limited availability of patient's tissues, suitable for transplants, damaged organs repair and regeneration is problematic. Therefore, there is an ongoing interest in the development of new materials that can be used as scaffolds for tissue regeneration. In particular, for bone tissue regeneration, scaffolds should match different requirements to obtain an appropriate bone-engineered tissue. Among them, the most important is related to interconnected pores with suitable size to allow cell proliferation and differentiation. Our approach was to develop a biointegrable scaffolds for bone tissue regeneration, providing the mechanical support for cell anchorage and new bone tissue deposition in the short-to-medium term, due to the CaPs nucleated onto the pore walls of the PU foam. The proposed PU porous

structure is expected, in the short time, to be engulfed in the newly formed bone tissue showing biodegradation only at long implantation time, without the production of any cytotoxic products [50]. On the other hand, several studies [51,52] have proved the influence of calcium phosphates on MSCs morphology, attachment and proliferation by using gelatin/β-tricalcium phosphate (TCP) [52] or hydroxyapatite/TCP composite scaffolds [51]. Among possible matrices, polyurethanes are a good choice due to their ability to present a wide range of structures and properties. The effect of polyurethanes design on pro-liferation, osteoblastic differentiation and calcification of bone marrow stromal cells has been already reported [25].

As stated in previous researches [36–38], the formation of a calcium phosphate phase similar to natural bone apatite on the surface of synthetic materials is an essential requirement for exhibiting a bone-bonding behaviour. Generally, the formation of the apatite-like layer needed to enhance the bone-bonding behaviour does not occur spontaneously on synthetic polymers, and a pre-treatment is necessary to activate the surfaces of polymers [53,60]. Using bioactive glass can be the simplest way for the nucleation and growth of CaPs layer on the surfaces of polymeric structures [38,40]. Another approach is the use of negatively charged surfaces as precursor for the nucleation of hydroxyapatite (HA) in a supersaturated Simulated Body Fluid (SBF) solution [54]. In the present study, PU foams were synthesized to develop a biointegrable matrix for preparation of porous composite scaffold containing osteoinductive and osteoconductive inorganic salt (HA) via nucleation treatment.

3.2. Morphological characterization

PU foam specimens before and after HA nucleation treatment were observed by SEM. The micrographs of the surface and cross-section of the PU foam (Fig. 2a, b) showed pores with a homogenous size and distribution. Representative SEM images of PU-4W showed the apatite layer nucleation and growth onto the PU foam surface (Fig. 2c, e) and the induction of apatite growth into the bulk of the foam, confirmed by the analysis on the cross-section (Fig. 2d, f). By a qualitative observation, the presence of nucleated HA appeared higher at the surface (Fig. 2c) than in the inner pore walls of the foam (Fig. 2d). Comparing the CaPs nucleation on the PU foam at the considered time-points (Fig. 3), an entangled network of plate-like HA crystals with thickness of about 100 nm can be observed. In addition, from 1 week to 4 weeks treatment, the morphology of the apatite crystal remained the same (i.e. plate-like), but the pore wall surface was more homogeneously coated, increasing the width and the size of the HA plates increasing the nucleation time.

3.3. Physical characterization

3.3.1. Density

The density evaluation (Fig. 4a) showed higher values by increasing the time of the nucleation treatment (i.e., from 1 to 4 weeks), compared to the untreated PU foam. In particular, a significant increase ($p < 0.05$) was detected only between 1 and 4 weeks of treatment, and between PU-4W and the untreated PU foam.

3.3.2. Water uptake

For the water uptake test, only PU-4W was selected due to presence of more apatite crystals when compared to other treated samples (i.e. higher density, Fig. 4a). In the water uptake (WU %) tests (Fig. 4b), different water absorption kinetics up to 48 h can be observed. In fact, the plateau was reached faster (i.e. after 6 h) for PU-4W and at low rate, after 48 h, for PU foam. PU-4W showed higher water absorption compared to PU foam in the first incubation time due to the presence of nano hydroxyapatite (nHA), which can absorb water quicker then PU alone. After reaching the plateau, no statistically differences in WU%were detected up to 8 days of incubation comparing PU and PU-4W.

3.4. Chemical characterization

After designing the PU foam with high open porosity and adequate pore dimension [33,34], its surface was activated for CaPs layer formation due to low potential of the PU foam for apatite formation. For this reason, calcium and phosphate ions have been exploited for formation of initial CaPs nuclei on the surface of pore walls, instead of the

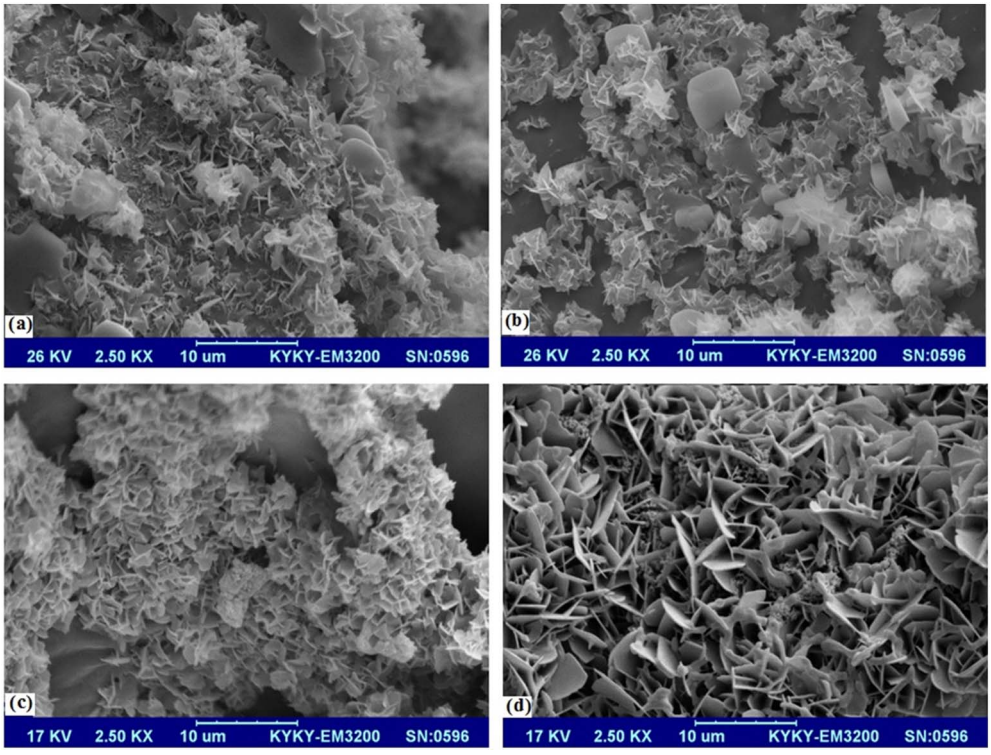

Fig. 3. SEM micrographs of CaPs nucleated on PU surface at the different time-points: a) PU-1W, b) PU-2W, c) PU-3W and d) PU-4W. Scale bar: 10 μm.

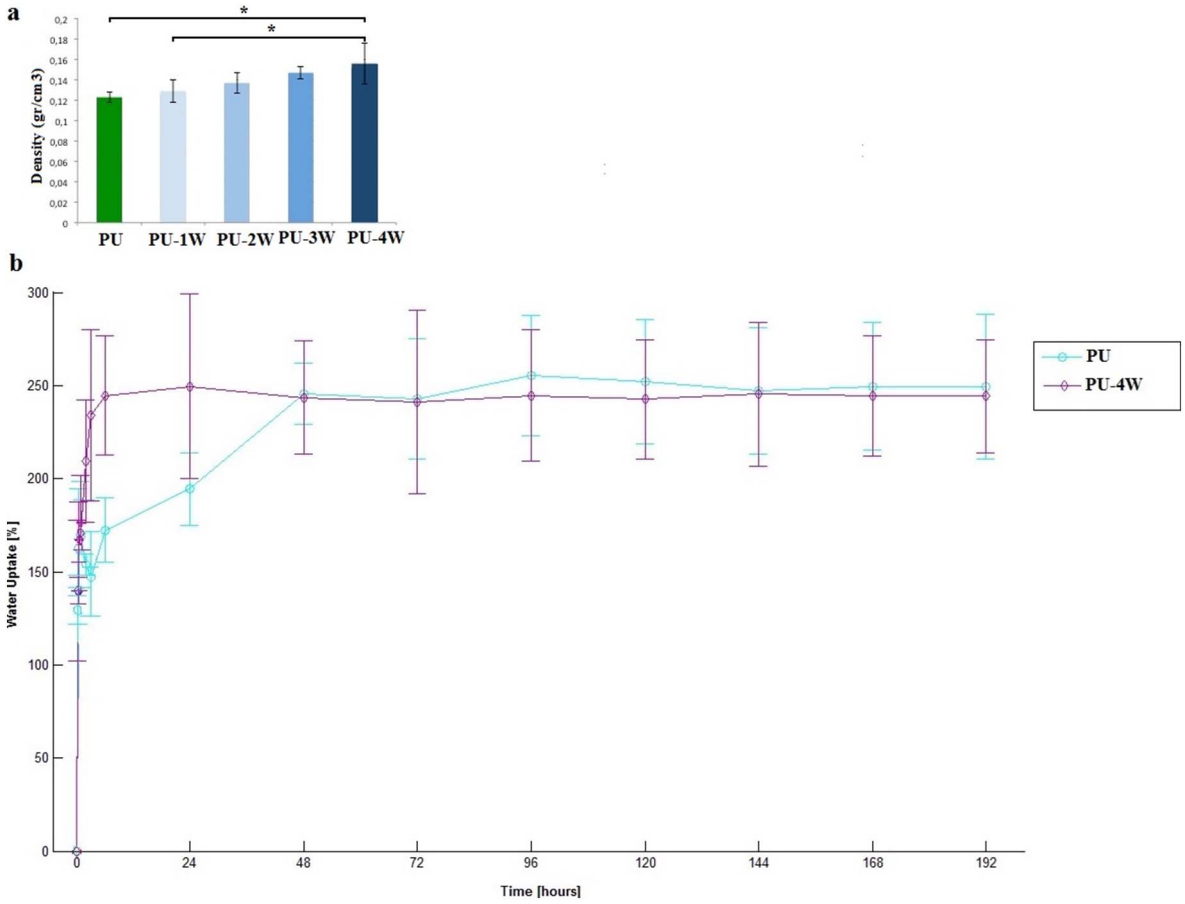

Fig. 4. a) Density values of PU and PU foams incubated from 1 to 4 weeks in SBF to obtain HA nucleation onto the pore walls of the PU foam, *: $p < 0.05$; b) Water uptake kinetics for PU foam and pU-4W.

bioactive glass commonly used for the activation of synthetic polymers surfaces (e.g., high molecular weight polyethylene, polyurethane, polycaprolactone) [38,55]. The CaPs can act as nucleation sites for apatite-like material formation and lead to further enhanced growth. After immersion of the PU foam samples in 1.5 SBF solution, the SBF can penetrate in the PU bulk structure, surface and pores, so that cal-cium and phosphate ions can interact with the polyurethane structure. In particular, the release of Ca^{2+} ions from SBF solution produces nucleation sites for the formation of apatite. The required ions for the apatite growth can diffuse to the nucleation site anisotropically, providing many nucleation sites causing an entangled network of plate-like HA crystals on the PU surface. The thickness of the HA crystals is about 100 nm, comparable to the crystal dimension and morphology of the physiological bone HA [56]. A possible mechanism in the development of the biomimetic reaction on the PU foam is related to the fact that the bone-like apatite crystals are formed via intermediate products of calcium phosphate. Some of the possible reactions in 1.5 SBF, considering its compositions [54], are as follows:

$$Ca^{2+} + HPO_4^{2-} + 2H_2O \rightarrow CaHPO_4 \cdot 2H_2O \text{ (DCPD)} \quad (3)$$

$$3\,Ca^{2+} + 2PO_4^{3-} \rightarrow Ca_3(PO_4)_2 \text{ (TCP)} \quad (4)$$

$$5\,Ca^{2+} + 3PO_4^{3-} + OH^- \rightarrow Ca_5(PO_4)_3OH \text{ (HA)} \quad (5)$$

where: DCPD = dibasic calcium phosphate dehydrate.

3.4.1. FTIR analysis

FTIR spectra of CaPs powders, obtained from treated PU foam samples (Fig. 5), showed the presence of functional groups attributed to hydroxyapatite. The characteristic band of out-of-plane bending (υ_4) of PO_4^{3-} was observed at 560–600 cm^{-1}. The weak band at 470 cm^{-1} can be assigned to the bending mode of phosphate (υ_2). Symmetrical stretching (υ_1) of PO_4^{3-} can be observed at 960 cm^{-1} and the bands at 1030–1100 cm^{-1} assigned to the asymmetric stretching of PO_4^{3-} (υ_3), bending and stretching modes of P—O vibrations are present at 600 and 1049 cm^{-1}, respectively. Besides that, a broad band related to the main vibration of symmetrical stretching (υ_1) of OH at 3566 cm^{-1}, joined with the bands at 3400 and 1629 cm^{-1} (H—O—H bond) were observed, possibly due to water absorption in CaPs coating [14,57]. In addition, no differences in the FTIR spectra were detected varying the weeks of nucleation treatment.

3.4.2. XRD analysis

All the diffraction peaks in XRD diffractograms acquired from the CaPs powders obtained by the treated PU foams (Fig. 6) can be assigned to monophase, low crystalline hydroxyapatite. Broadening of the peaks in XRD patterns pointed out to the small size and low crystalline HA, significant of a HA structure similar to that of the natural bone mineral [38,57]. Major peaks with 2θ values of 25.80, 31.64, 39.41, 46.69 and 49.29°, respectively corresponded to the (002), (211), (310), (222) and (213) planes of HA.

3.5. Mechanical characterization

Representative stress-strain curves for PU, PU-1W, and PU-4W are reported in Fig. 7, and the values of the considered mechanical parameters are reported in Table 2. For low strain value (0–0.2 mm/mm), the slope of the stress/strain curves obtained for the treated foams was higher than that of the untreated PU foam. In fact, E value was significantly higher than that of the PU one, reaching a double value for PU-4W sample. There is no significant difference ($p > 0.05$) between

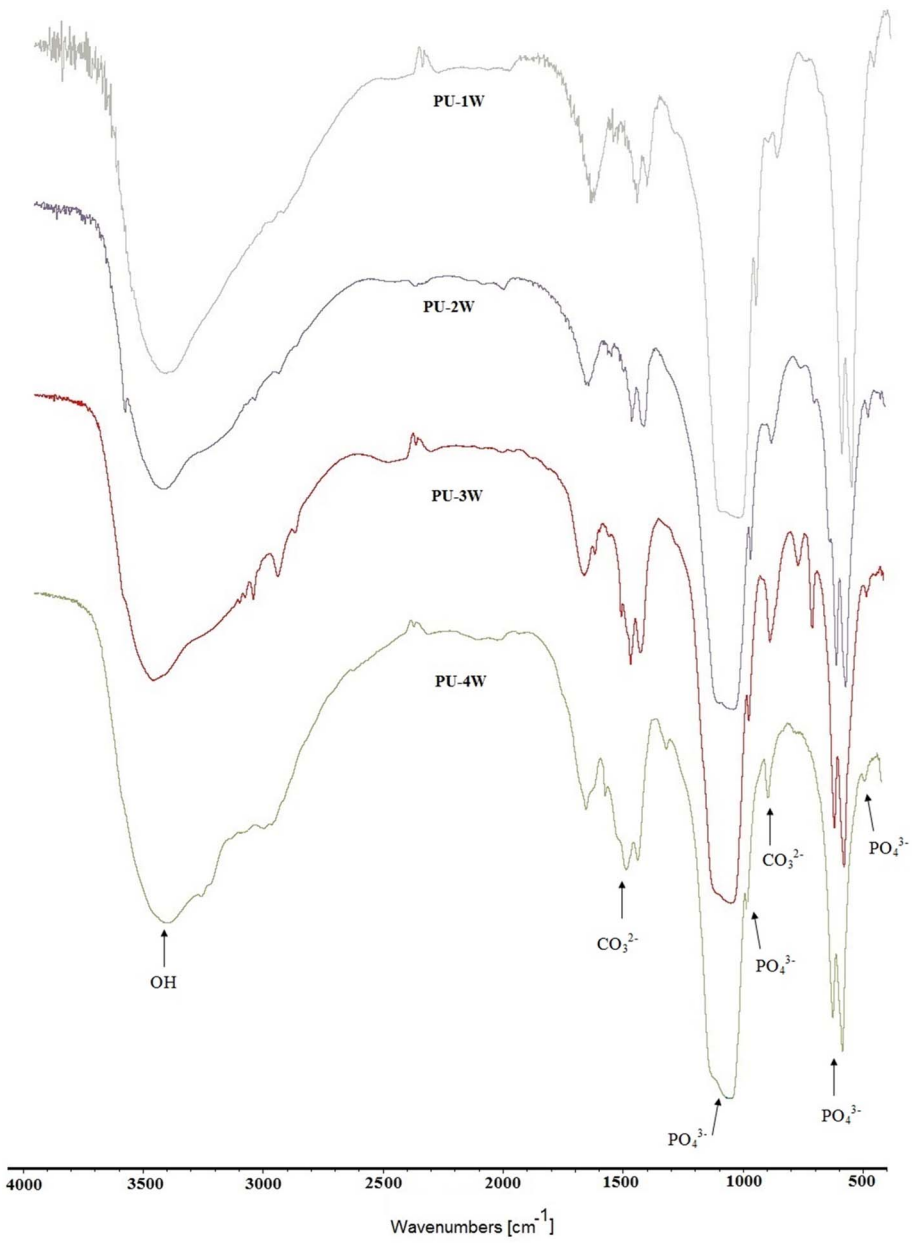

Fig. 5. FT-IR spectra of CaPs powders nucleated on the threated PU foams (PU-1W, PU-2W, PU-3W and PU-4W).

PU-1W, PU-2W and PU-3W, but PU-4W E value is significantly different ($p < 0.05$) from the others. In addition, the maximum stress of treated PU foams increased by increasing the treatment time (i.e., a higher value can be detected for PU-4W compared to PU-1W), showing a significant difference when compared to PU alone ($p < 0.05$). All foams showed similar ($p > 0.05$) residual deformation, indicating that the mineralization treatment did not influence strain recovery. In addition, PU-4W sample exhibited a higher hysteresis area in comparison to PU and PU-1W, indicating higher energy dissipation, probably caused by a larger amount of HA nucleated onto the pore walls of the PU foam and by the higher value of maximum stress reached during compression tests.

In this work, biomineralization caused a significant increase in the mechanical properties of the PU foams after 4 weeks treatment compared to the untreated sample. An explanation for that can be the chemical bond formation between calcium and negative groups of PU due to partially hydrolysis of foam after immersion in 1.5 SBF. The hydrolysis lead to the production of a hydrophilic end group such as carboxyl and hydroxyl groups, which can act as suitable binding sites for calcium ions, following phosphate attraction, initiating apatite nucleation and formation of HA layer by plate shape morphology, evidencing the substrate chemistry effect on the CaPs layer morphology [38]. Hence, the polar structure of PU due to partially hydrolysis, increases the adhesion of the apatite layer to the pore walls of the foam, finally improving the mechanical properties of the scaffold. Although neither untreated nor treated PU foams did reproduce the morphology and mechanical properties of mature trabecular bone, whose porosity ranges from 75 to 200 μm, PU-based scaffolds did meet several different requirements, such as easy shaping during surgical implantation. The mechanical properties of the scaffolds are considered as a less important factor because it is presumed that osteoblast differentiation, colonization and proliferation lead to CaPs deposition during extracellular matrix formation, so to improve PU foams mechanical strength [58].

3.6. In vitro cytocompatibility test

BMSCs isolated from rat were cultured on PU and PU-4W samples

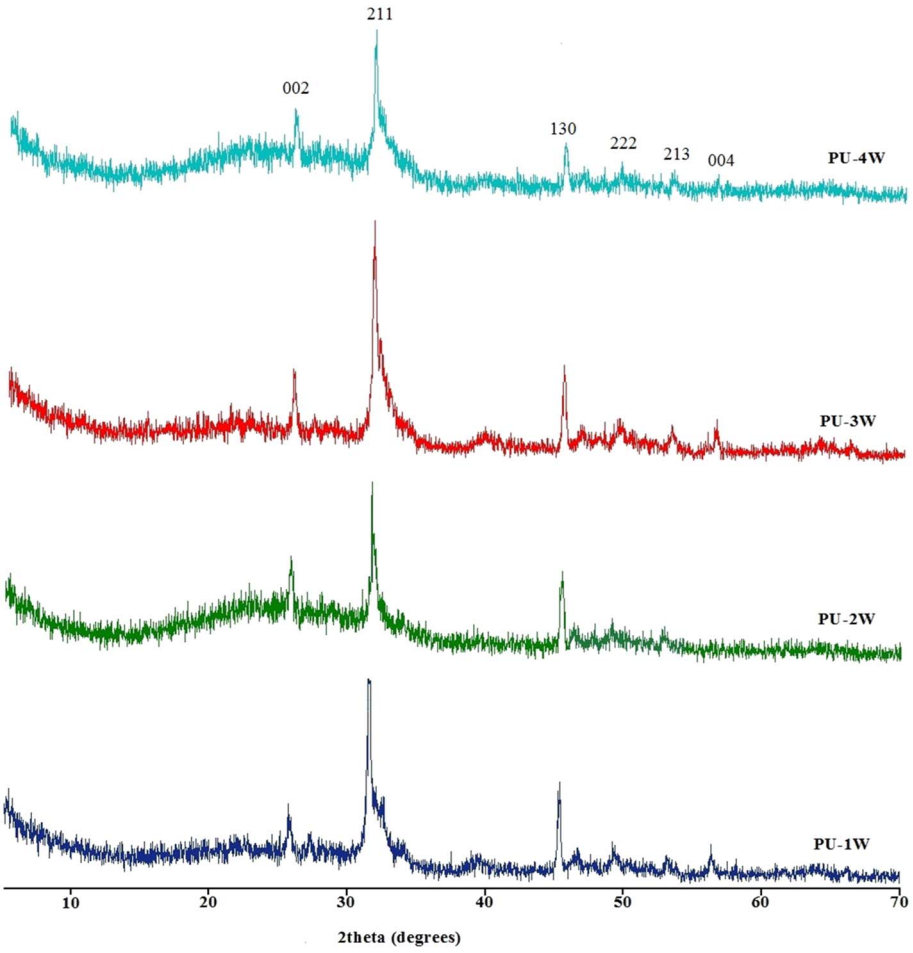

Fig. 6. XRD diffractograms of CaPs powders nucleated on the treated PU foams (PU-1W, PU-2W, PU-3W and PU-4W).

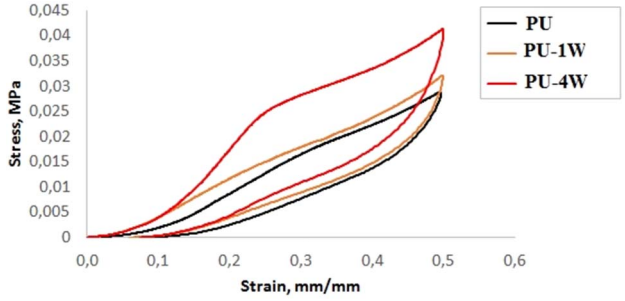

Fig. 7. Representative compressive stress/strain curves obtained for PU, PU-1W and PU-4W tested in wet condition.

Table 2
Compressive mechanical parameters for untreated and treated PU foams.

Wet	E [kPa]	σ_{max} [kPa]	ε_r [%]	Hysteresis Area [mJ/cm^3]
PU	13.75 ± 1.06	30.56 ± 2.76	7.22 ± 1.2	3.07 ± 0.31
PU-1W	15.67 ± 3.95	37.03 ± 0.93	6.39 ± 0.51	3.74 ± 0.98
PU-2w	16.27 ± 2.66	43.7 ± 1.38	9.11 ± 0.14	4.08 ± 1.03
PU-3W	17.8 ± 5.99	42.34 ± 0.50	7.53 ± 0.52	3.96 ± 0.50
PU-4W	25.40 ± 5.84	49.47 ± 0.95	6.25 ± 0.84	4.33 ± 0.50

up to 14 days, using TCPS as control. Both scaffolds promoted cell viability, exhibiting after 3 days of culture the same value detected for TCPS ($p > 0.05$, Fig. 8). However, viability of cells cultured on PU-4W significantly increased up to 115% compared to PU and TCPS 7 days after seeding ($p < 0.05$), but no significant difference ($p > 0.05$) was evidenced after 14 days of culture. So, based on cytocompatibility tests, both untreated and treated PU foams are as compatible as the TCPS surface used as control. The obtained results are comparable with other in vitro cytocompatibility tests previously performed on PU foams having the same composition [4,33,35,48,49] of the PU foams tested in this research work. SEM images acquired for PU-4W, 24 h after seeding (Fig. 9b), showed a better cell adhesion on the surface compared to PU (Fig. 9a). Increasing culture time, cell attachment improved on the surface of both scaffolds (Fig. 9c-f). However, cells on PU-4W formed long cytoplasmatic branches and interacted with pore walls, due to the surface biomineralization that provided desirable attachment sites for BMSCs. In addition, cells became well spread after 24 h, better adhering onto the nHA coated pore walls in comparison to the smooth PU wall surface (Fig. 10 a-d).

Zanetta et al. [48] investigated proliferation of human MSCs on PU foam and observed a good cells adhesion and biomineralization due to ECM deposition, as detected in the present work on PU-4W. These results demonstrate that both PU and PU-4W scaffolds provided the cells with the necessary support to adhere and proliferate. Interestingly, the biomimetic surface modification here proposed provided a more desirable surface for cell attachment and proliferation compared to TCPS and untreated PU scaffold. The amount of released ALP (Fig. 11) increased for both PU scaffolds and composites during the whole culture time up to 14 days. However, no significant difference ($p > 0.05$) comparing untreated and treated PU scaffolds was observed for the considered time-points, as well as among the PU-based scaffolds and TCPS used as control group. These results revealed that cells cultured onto the scaffolds (even when nHA nucleated on the pore wall surface), in the absence of any osteogenic stimulation media, promoted ALP activity similar to the control group.

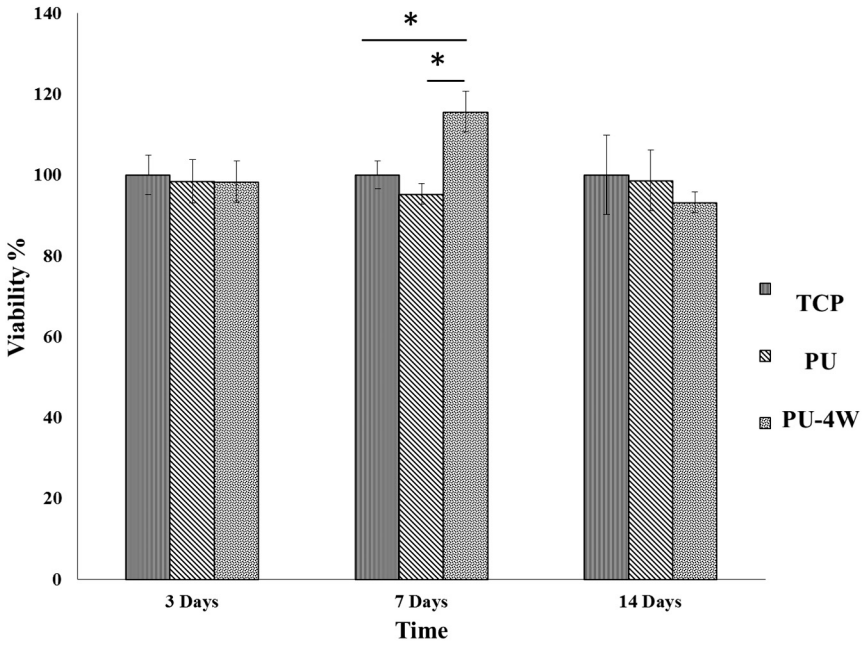

Fig. 8. Relative cell viability of BMSCs cultured on PU and PU-4W foams at the three considered time points. * = $p < 0.05$.

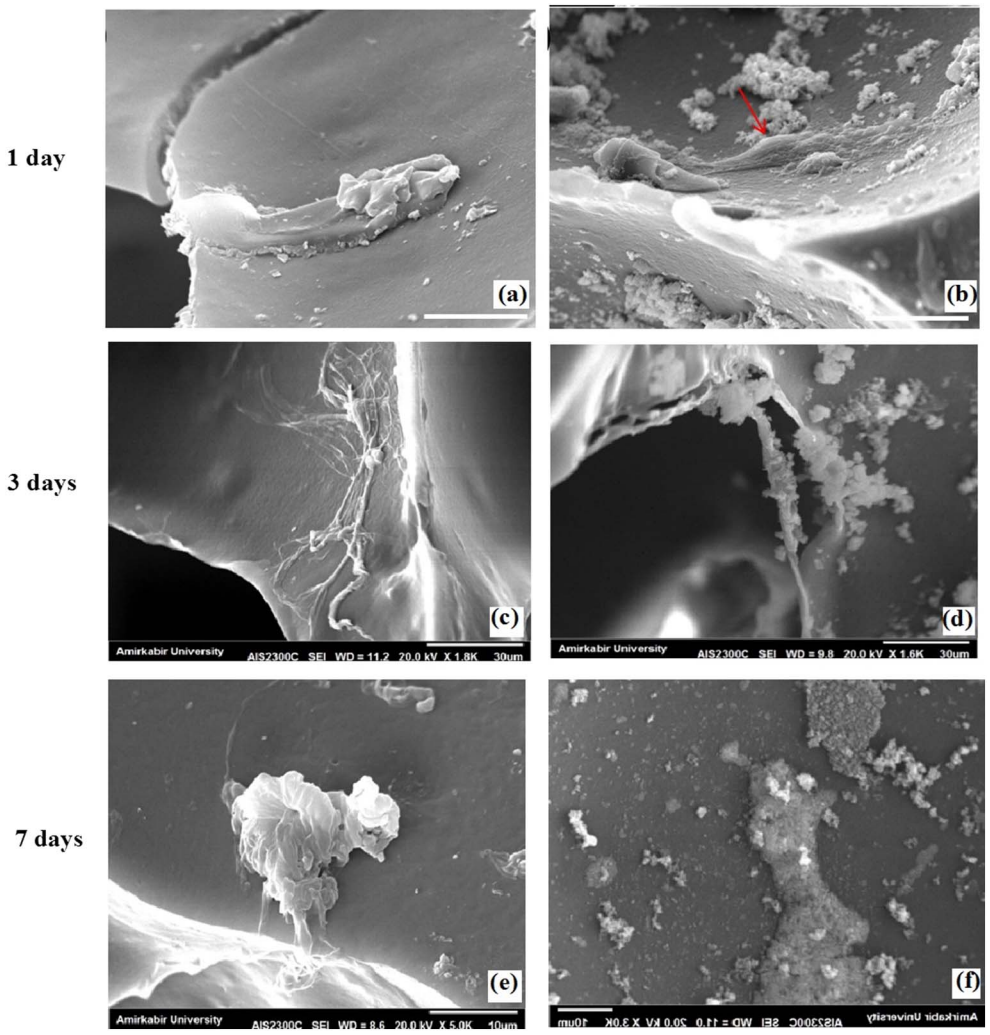

Fig. 9. SEM micrographs of PU and PU-4W foams seeded with BMSCs and cultured for a, b) 1 day; c, d) 3 days and e, f) 7 days. Red arrow represents cell spread on the pore surface. Scale bar: 500 µm (a, c, e), 30 µm (b, d, f). (For interpretation of the references to color in this figure legend, the reader is referred to the web version of this article.)

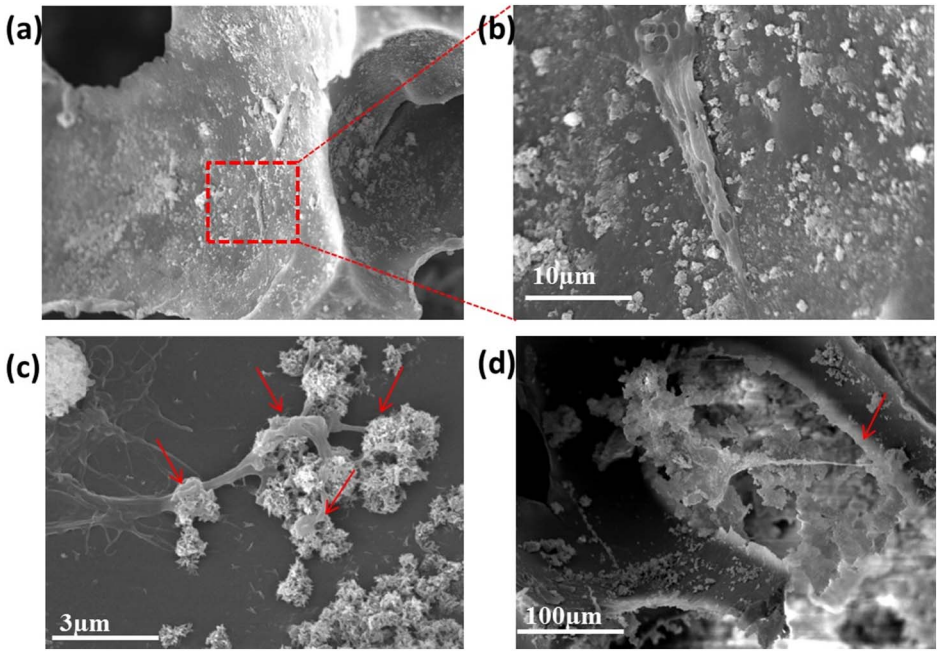

Fig. 10. SEM micrographs of PU-4W foams seeded with BMSCs and cultured for 24 h. Cells spread on the scaffold surface (a, b) and filopodia adhered to HA nanoplates (c). Cells could interact with pore walls and form bridge from one side to other side (d, red arrow). Scale bar: 10 µm (a, b), 3 µm (c) and 100 µm (d). (For interpretation of the references to color in this figure legend, the reader is referred to the web version of this article.)

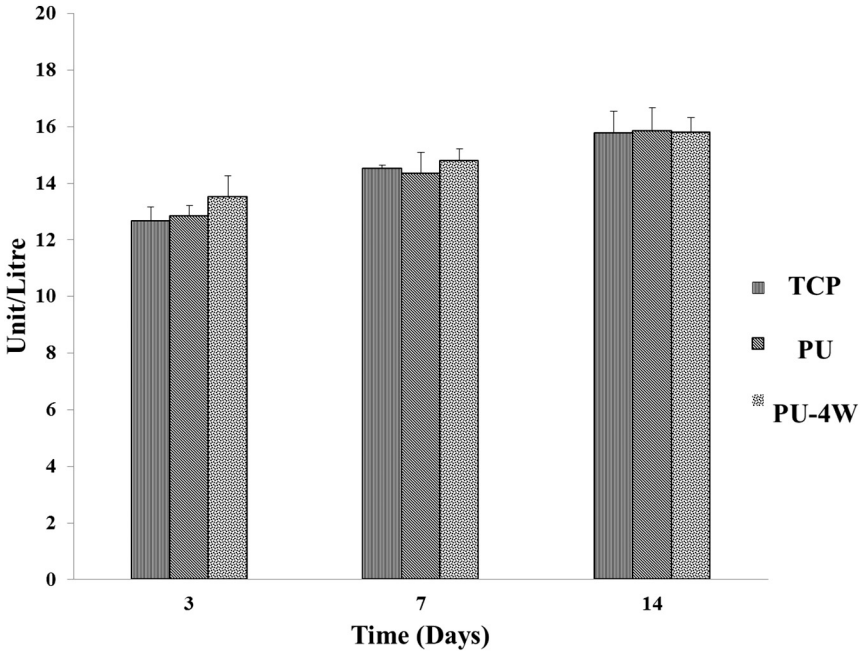

Fig. 11. ALP values obtained by BMSCs culture onto PU and PU-4W scaffolds at the considered time points.

4. Conclusions

Biomineralization of PU foams can be very useful in the development of materials for cancellous bone replacement, regarding to their morphological properties, ability to promote BMSCs cell adhesion and proliferation. The method here proposed for the nucleation of nano hydroxyapatite onto the surface of the PU foam walls appeared adequate for improving cells adhesion, significantly increasing the compressive mechanical properties of the scaffold. Further improvements of BMSCs performance on PU foam scaffold can be achieved by inducing greater in situ formation of apatite on PU structure, incorporation of CaPs fillers, and in vitro cell culture under dynamic condition such as perfusion chambers, bioreactors and electromagnetic stimulation.

Acknowledgements

This project was financially supported by the grant (2012-0842) from the Cariplo Foundation 2012 Program.

References

[1] N.L. Leong, H.H. Lu, Conf. Proc. IEEE Eng. Med. Biol. Soc. 1 (2006) 2651–2654.
[2] C.W. Kim, R. Talac, L. Lu, M.J. Moore, B.L. Currier, M.J. Yaszemski, J. Biomed. Mater. Res. A 85 (4) (2008) 1114–1119.
[3] X. Shi, B. Sitharaman, Q.P. Pham, F. Liang, K. Wu, W. Edward Billups, et al., Biomaterials 28 (28) (2007) 4078–4090.
[4] M.C. Tanzi, S. Farè, P. Petrini, A. Tanini, E. Piscitelli, S. Zecchi Orlandini, et al., J. Appl. Biomater. Biomech. 1 (1) (2003) 58–66.
[5] I. Torigoe, S. Sotome, A. Tsuchiya, T. Yoshii, M. Takahashi, S. Kawabata, et al., Cell Transplant. 16 (7) (2007) 729–739.
[6] K. Song, T. Liu, Z. Cui, X. Li, X. Ma, J. Biomed. Mater. Res. A 86 (2) (2008) 323–332.
[7] J.E. Schroeder, R. Mosheiff, Injury 42 (2011) 609–613.

[8] K.T. Shalumon, N.S. Binulal, N. Selvamurugan, S.V. Nair, D. Menon, T. Furuike, Carbohydr. Polym. 77 (2009) 863–869.
[9] F.R. Rose, R.O. Oreffo, Biochem. Biophys. Res. Commun. 292 (2002) 1–7.
[10] G. Tetteh, A.S. Khan, R.M. Delaine-Smith, G.C. Reilly, I.U. Rehman, J. Mech. Behav. Biomed. Mater. 39 (2014) 95–110.
[11] G. Shaohua, Z. Ning, W. Lu, Y. Meijiao, L. Hong, S. Aimei, H. Jing, W. Guancong, Y. Pishan, Int. J. Med. 7 (2012) 5405–5414.
[12] J. Venugopal, S. Low, A.T. Choon, T.S. Sampath Kumar, S. Ramakrishna, J. Mater. Sci. Mater. Med. 19 (5) (2008) 2039–2046.
[13] S.S. Olmez, P. Korkusuz, H. Bilgili, S. Senel, Pharmazie 62 (6) (2007) 423–431.
[14] M. Sadjadi, M. Meskinfam, B. Sadeghi, H. Jazdarreh, K. Zare, J. Biomed. Nanotechnol. 7 (2011) 450–454.
[15] J. Kim, I.S. Kim, T.H. Cho, K.B. Lee, S.J. Hwang, G. Tae, et al., Biomaterials 28 (10) (2007) 1830–1837.
[16] D.A. Wahl, J.T. Czernuszka, Eur. Cell. Mater. 11 (2006) 43–56.
[17] X.N. Qi, Z.L. Mou, J. Zhang, Z.Q. Zhang, J. Biomed. Mater. Res. A 102 (2) (2014) 366–372.
[18] S.P. Uswatta, I.U. Okeke, A.C. Jayasuriya, Mater Sci Eng C Mater Biol Appl 69 (2016) 505–512.
[19] P.A. Gunatillake, R. Adhikari, Eur. Cell Mater. 5 (2003) 1–16.
[20] J. Ren, T. Ren, P. Zhao, Y. Huang, K. Pan, J. Biomater. Sci. Polym. Ed. 18 (5) (2007) 505–517.
[21] H. Nie, C.H. Wang, J. Control. Release 120 (1–2) (2007) 111–121.
[22] S.S. Kim, M.S. Park, S.J. Gwak, C.Y. Choi, B.S. Kim, Tissue Eng. 12 (10) (2006) 2997–3006.
[23] H.W. Liu, C.H. Chen, C.L. Tsai, I.H. Lin, G.H. Hsiue, Tissue Eng. 13 (5) (2007) 1113–1124.
[24] J. Zhang, B.A. Doll, E.J. Beckman, J.O. Hollinger, J. Biomed. Mater. Res. A 67 (2) (2003) 389–400.
[25] K.D. Kavlock, T.W. Pechar, J.O. Hollinger, S.A. Guelcher, A.S. Goldstein, Acta Biomater. 3 (4) (2007) 475–484.
[26] I.C. Bonzani, R. Adhikari, S. Houshyar, R. Mayadunne, P. Gunatillake, M.M. Stevens, Biomaterials 28 (3) (2007) 423–433.
[27] J. Zhang, E.J. Beckman, N.J. Piesco, S. Agarwal, Biomaterials 21 (2000) 1247–1258.
[28] J. Zhang, E.J. Beckman, J. Hu, G. Yuang, S. Agarwal, J.O. Hollinger, Tissue Eng. 8 (5) (2002) 771–785.
[29] K. Gorna, S. Gogolewski, J. Biomed. Mater. Res. 67A (2003) 813–827.
[30] S. Gogolewski, K. Gorna, J. Biomed. Mater. Res. 80A (2007) 94–101.
[31] S.A. Guelcher, A. Srinivasan, A.E. Hafeman, K.M. Gallagher, S. Khetan, et al., Tissue Eng. 13 (9) (2007) 2321–2333.
[32] S.A. Guelcher, V. Patel, K. Gallagher, S. Connolly, J.E. Didier, et al., Tissue Eng. 12 (5) (2006) 1247–1259.
[33] S. Farè, P. Petrini, M.C. Tanzi, EUROMAT, Biomaterials 6 (2001) 1–7.
[34] S. Farè, P. Petrini, M.C. Tanzi, A. Bigi, N. Roveri, D. Mantovani (Ed.), Advanced Materials for Biomedical Application, Canadian Institute of Mining, Metallurgy and Petroleum, Montréal, 2002, pp. 17–26.
[35] I. Dal Prà, P. Petrini, A. Charini, S. Bozzini, S. Farè, U. Armato, Tissue Eng. 9 (6) (2003) 1113–1121.
[36] L. Hench, J. Am. Ceram. Soc. 74 (1991) 1487–1510.
[37] R. Z. Legeros, I. Orly, M. Gregoire, G. Daculsi, J. E. Davies (ed), University of Toronto Press, Toronto, 1991, p. 76.
[38] R.L. Reis, A.M. Cunha, J. Mater. Sci. Mater. Med. 8 (1997) 897–905.
[39] W. Li, Y. Ding, S. Yu, Q. Yao, A.R. Boccaccini, ACS Appl. Mater. Interfaces 7 (37) (2015) 20845–20854.
[40] L. Hench, Chem. Ind. 17 (1995) 547–550.
[41] P. Li, X. Ye, I. Kangasniemi, J. Blieckhogervorst, C. Klein, K. Groot, J. Biomed. Mater. Res. 29 (1995) 325–328.
[42] A.A. Campbell, G. Fryxell, J. Linehan, G. Graff, J. Biomed. Mater. Res. 32 (1996) 111–118.
[43] T. Kokubo, K. Hata, T. Nakamura, T. Yamamuro, 4, W. Bonfied, G. W. Hastings and K. E. Tanner (eds), Butterworth-Heineman, London, 1991,p. 113.
[44] M. Tanahashi, T. Yao, T. Kokubo, M. Minoda, T. Miyamoto, T. Nakamura, T. Yamamuro, J. Mater. Sci. Mater. Med. 6 (1995) 319–326.
[45] S.H. Li, Q. Liu, J.R. Wijn, B.L. Zhou, K. De Groot, Biomaterials 18 (1997) 389–395.
[46] Z.G. Thang, S.H. Teoth, W. McFarlane, L.A. Poole-Warren, M. Umezu, Mater Sci Eng C Mater Biol Appl 20 (2002) 149–152.
[47] C.A. Martinez-Perez, P.E. Garcia-Casillas, A. Martinez-Villafane, J. Romero-Garcia, Silicon Chem. 2 (2003) 179–184.
[48] M. Zanetta, N. Quirici, F. Demarosi, M.C. Tanzi, L. Rimondini, S. Farè, Acta Biomater. 5 (2009) 1126–1136.
[49] S. Bertoldi, S. Farè, M. Denegri, D. Rossi, H.J. Haugen, O. Parolini, M.C. Tanzi, J. Mater. Sci. Mater. Med. 21 (2010) 1005–1011.
[50] S. Bertoldi, S. Farè, M. Moscatelli, A. Addis, F. Vitari, C. Domeneghini, M.C. Tanzi, ISBN: 9788880800859, Faenza, RA, Italy, 2008, 120–127.
[51] Y. Takahashi, M. Yamamoto, Y. Tabata, Biomaterials 26 (2005) 3587–3596.
[52] L. Livingston, S. Gordon, M. Archambauld, S. Kadiyala, K. Mcintosh, A. Smith, et al., J. Mater. Sci. Mater. Med. 14 (2003) 211–218.
[53] R. Nirmala, K. Taek Nam, R. Navamathavan, S. Park, H. Kim, Nanoscale Res. Lett. 6 (2011) 2.
[54] Z. Peixin, M. Yoshitake, K. Kunihito, Biomaterials 25 (2004) 3915–3921.
[55] M. Bil, J. Ryszkowska, J. Roether, O. Bretcanu, A. Boccaccini, Biomed. Mater. 2 (2007) 93–101.
[56] N. Chengyun, C. Haimei, Z. Wenjun, Y. Zhaoyi, C. Hao, Z. Huade, L. Shumei, Y. Shiheng, T. Guoxin, Appl. Surf. Sci. 255 (2008) 429–431.
[57] M.S. Sadjadi, M. Meskinfam, B. Sadeghi, H. Jazdarreh, K. Zare, Mater. Chem. Phys. 124 (2010) 217–222.
[58] S. Farè, P. Petrini, S. Bozzini, L. Draghi, M.C. Tanzi, Transactions of 18th European Society of Biomaterials Conference, 1–4 October, 2003, Stuttgart, Germany, (2013).
[59] S. Bertoldi, S. Farè, H.J. Haugen, M.C. Tanzi, J. Mater. Sci. Mater. Med. 26 (5) (2015) 182.
[60] H. Chen Guo, E. Ye, Z. Li, M.Y. Han, X.J. Loh, Mater. Sci. Eng. C 70 (2017) 1182–1191.
[61] Z. Li, E. Ye, David, R. Lakshminarayanan, X.J. Loh, Small 12 (35) (2016) 4782–4806.
[62] R. Lakshminarayanan, X.J. Loh, S. Gayathri, S. Sindhu, Y. Banerjee, R.M. Kini, S. Valiyaveettil, Biomacromolecules 7 (11) (2006) 3202–3209.
[63] R. Lakshminarayanan, E. Ooi Chi-Jin, X.J. Loh, R. Manjunatha Kini, S. Valiyaveettil, Biomacromolecules 6 (3) (2005) 1429–1437.